THE GLYPICAN DALLY IS A TARGET AND MEDIATOR OF BMP SIGNALING IN EGGSHELL PATTERNING

by

DAVID JAMES LEMON

A thesis submitted to the

Graduate School - Camden

Rutgers, The State University of New Jersey

in partial fulfillment of the requirements

for the degree of Master of Science

Graduate program in Biology

written under the direction of

Dr. Nir Yakoby

and approved by

_____

Nir Yakoby

_____

Joseph V. Martin

_____

Daniel H. Shain

Camden, New Jersey

May 2012

ABSTRACT OF THE THESIS

The glypican Dally is a target and mediator of BMP signaling in eggshell patterning

By DAVID JAMES LEMON

Thesis Director:
Dr. Nir Yakoby

Heparan sulfate proteoglycans (HSPGs) participate in the regulation of numerous cell signaling pathways in tissues throughout animal development. In *Drosophila melanogaster*, the HSPG Division-abnormally-delayed (Dally) acts as a co-receptor in several signaling pathways, including bone morphogenetic protein (BMP) signaling, during imaginal wing disc development. Previously, it has been shown that *dally* is patterned in the follicle cells (FCs), a mono-layer of epithelial cells which surrounds the oocyte. These cells derive the formation of the eggshell. We found this pattern to be evolutionary conserved across *Drosophila* species. Also, *dally*'s pattern spatially overlaps the BMP signaling domain, which was monitored by phosphorylated-Mothers-against-Dpp (P-MAD). Using genetic perturbations, we determine that in the FCs, *dally* is a downstream target of BMP signaling. Furthermore, in clones of cells null for *dally*, P-MAD is lost cell autonomously. When *dally* was perturbed uniformly throughout the FCs the BMP signaling gradient was expanded or restricted in gain-of-function or loss-of-

function, respectively. Consequently, the FCs patterning shifted along the anterior-posterior axis. Perturbing *dally* in the anterior domain of the FCs resulted in changes of eggshell morphology. Specifically, the depletion of *dally* results in an overall increase in operculum length. Based upon our results, and consistent with Dally's role in wing imaginal discs, we propose a model by which Dally contributes to eggshell patterning along the anterior-posterior axis by regulating BMP signaling.

TABLE OF CONTENTS

SECTIONS

LIST OF FIGURES

LIST OF GRAPHS

Introduction

*Drosophila o*ogenesis:

The *Drosophila melanogaster* eggshell is a well-established and convenient model for studying intercellular signaling and tissue patterning (Berg, 2005; Horne-Badovinac and Bilder, 2005). During oogenesis, developing egg chambers progress through fourteen morphologically defined stages over the course of three days (Fig. 1 A) (Spradling, 1993). During stage 10, midway through oogenesis, the developing egg, called an egg chamber, is composed of three main compartments (Fig. 1 B). The oocyte, which will become the embryo after fertilization, makes up the bulk of the posterior half of the egg chamber. The oocyte is surrounded by a monolayer of epithelial cells called the follicle cells (FCs) which will ultimately give rise to the eggshell. Finally, to the anterior of the oocyte are the nurse cells which provide nutrients to the growing oocyte. Nurse cells are surrounded by a layer of flat epithelial cells called the stretch cells.

The *Drosophila* eggshell:

The mature eggshell surrounds the developing embryo and is produced by the FCs near the end of oogenesis. The eggshell is made up of chorion proteins, and possesses a handful of three dimensional structures on its dorsal-anterior (Fig. 1 C). These include tube-like structures called the dorsal appendages (DAs) which allow for gas exchange, a weakened structure called the operculum, which serves as an escape hatch for the larvae. At the most anterior domain, a cone-shaped micropyle serves as

an entry point for sperm during fertilization (Berg, 2005; Shravage et al., 2007). These three dimensional structures are highly sensitive to modifications in the levels of cell signaling pathways, and I will focus on the morphological changes in the operculum.

Intercellular signaling pathways:

During oogenesis the FCs receive input from a several signaling pathways including the bone morphogenetic protein (BMP) (Twombly et al., 1996; Dobens and Raftery, 2000; Parker et al., 2004; Massague and Gomis, 2006), the epidermal growth factor receptor (EGFR) (Neuman-Silberberg and Schupbach, 1994), among others. Here I focus on the BMP signaling. The BMP pathway, during early and mid-stages of oogenesis, is largely responsible for controlling patterning along the anterior-posterior axis (Neuman-Silberberg and Schupbach, 1994; Berg, 2005).

Signaling in the BMP pathway begins when the BMP4-like ligand, Decapentaplegic (Dpp) (Padgett et al., 1987; Parker et al., 2004), binds to a complex of Type I and Type II BMP receptors. This complex is internalized and phosphorylates the intracellular mediator Mothers-against-Dpp (Mad) to become P-Mad. Then, together with Medea (Med) they translocate, into the nucleus, and function as a transcription factor (Fig. 2 A) (Baker and Harland, 1997; Wu and Hill, 2009).

In oogenesis, Dpp is secreted from the stretch cells and the anterior-most, centripetally migrating FCs (Twombly et al., 1996) to generate a gradient from anterior to posterior (Fig. 2 B). Initially, the tkv receptor is expressed uniformly throughout the FCs, and interacts with the anterior source of Dpp, which forms a ring of 2-3 cell rows of

P-Mad at the anterior FCs (Twombly et al., 1996; Dobens and Raftery, 2000; Niepielko et al., 2011) (Model shown in Fig. 2 C).

The FCs are a monolayer epithelial sheet at stage 10 (Spradling, 1993), approximately halfway through oogenesis, but over the remaining day and a half of development will move and change shape, eventually giving rise to the various three dimensional structures of the eggshell (Berg, 2008). The FCs do so based upon positional information they receive during earlier stages, which ultimately pattern this tissue, and determine a cell's fate.

Tissue patterning:

The most prominent of the eggshell's structures are the DAs. These are formed from two adjacent populations of cells (Berg, 2005; Berg, 2008). The top part of these structures comes from the cells which at stage 10B express a high level of the transcription factor Broad (BR) (Fig. 3 A, red) (Tzolovsky et al., 1999). Adjacent to the BR domains are two "L" shaped populations of cells (Fig. 3 A, green) which express the protease Rhomboid (Rho) (Ruohola-Baker et al., 1993). These cells will give rise to the bottom part of the future dorsal appendage (Berg, 2008; Yakoby et al., 2008a). In between and toward the anterior from these BR and Rho domains is a clearing in BR expression (Fig. 3 A, B in red). This clearing, which expresses Fasciclin III, a cell surface protein, is known as the midline domain, is fated to become the eggshell's operculum (Fig. 3 C). The operculum is subdivided into three zones which come from divisions of this midline domain (Fig. 3 B, D) (Shravage et al., 2007).

The role of glypicans in tissue patterning:

Division-abnormally-delayed (Dally) is one of several extensively glycosylated proteoglycans (Esko and Zhang, 1996) which are highly conserved in animals (Kooyman et al., 1995; Salmivirta et al., 1996). Heparan sulfate proteoglycans (HSPGs) such as Dally consist of a protein core and long branched chains of heparan sulfate (Kirkpatrick et al., 2006). HSPGs are classified into groups based upon the mechanism with which they are tethered to the cell membrane (Lander et al., 1996). Dally is one of the glypican subset of HSPGs, as it is attached to the cell membrane via a glycosylphosphatidylinositol (GPI) linkage (Edidin et al., 1991; Lander et al., 1996).

Glypicans, including Dally and a similar molecule, Dally-like (Dlp), have previously been shown to interact with the morphogen gradients of several signaling pathways in other tissues, including the BMP (Jackson et al., 1997; Belenkaya et al., 2004; Akiyama et al., 2008; Vuilleumier et al., 2010; Raftery and Umulis, 2012), EGFR (Baeg et al., 2001; Wang et al., 2008; Pizette et al., 2009; Yan et al., 2009), Wingless (Baeg et al., 2001; Blair, 2005; Yan et al., 2009), and Hedgehog (Han et al., 2004; Lin, 2004; Takeo et al., 2005; Eugster et al., 2007). Additionally, in humans, glypican malregulation has been implicated in a handful of cancers (Matsuda et al., 2001; Ding et al., 2005).

Dally could possibly affect change in tissue patterning by altering the diffusion rates of morphogens, sequestering ligands on the cell membrane, or by functioning as a necessary coreceptor. If any of these options is indeed the case, perturbations of *dally* will modify morphogen gradients, tissue patterning that will lead to morphological changes.

dally is expressed in a pattern that is evolutionarily conserved across *Drosophila* species. It is a downstream target of BMP signaling, and is also involved in both the patterning of the FCs and eggshell morphogenesis.

Materials and Methods

Flies:

Drosophila melanogaster stocks include wild-type (OreR), UAS-dpp (a gift from T. Schüpbach), UAS-tkv* (Lecuit et al., 1996), UAS-*dad* (Tsuneizumi et al., 1997), UAS-Dally^{strong} (H. Nakato), UAS-RNAiDally (Vienna Drosophila Research Center), UAS-shDally (Hudson and Cooley, Transgenic RNAi Project), CY2-GAL4, E4-GAL4, GR1-GAL4 (Duffy, 2002). The *Drosophila* species *D. willistoni* (The San Diego Stock Center) and *D. nebulosa* (a gift from D. Stern) were also used. All flies were maintained at 23C on standard high-agar cornmeal media, activated yeast was added to fly vials 18-30 hours prior to dissection and continuously during egg collection.

Genetic tools:

The GAL4/UAS allowed for targeted misexpression of *dally* constructs. By crossing a fly which produces the yeast transcription factor GAL4 in a specific tissue and time, with a fly which contains a gene of interest with an upstream activating sequence (UAS), *dally* was depleted or overexpressed (Fig. 10) (Muqit and Feany, 2002).

Mosaic analysis of Dally's effect on BMP signaling was conducted with the FLP/FRT mitotic recombination system (Xu and Rubin, 1993; Duffy, 2002) and FRT^{2A} Dally^{80} (Crickmore and Mann, 2006). This system allows for the creation of mosaic epithelial tissue, by recombining sequences between flippase (FLP) recognition targets

(FRTs), which makes observing the effects of loss-of-function perturbations of *dally,* an otherwise lethal mutation, possible (St Johnston, 2002).

RNA *in situ* hybridizations:

In situ hybridization was done as previously described (Wang et al., 2006; Yakoby et al., 2008a). Ovaries were dissected in cold Grace's medium for ≤15 minutes and fixed with 4% paraformaldehyde in heptane, DMSO, 0.2% Tween and PBS, dehydrated with washes of progressively increasing concentrations of methanol, and stored at -20C. Tissue was prehybridized for three hours at 60C in pre-hybridization solution followed by overnight hybridization at 65C using 1:10 digoxygenin-labeled probe in hybridization buffer. Then tissue was blocked in 1% BSA for one hour at room temperature. Pre-adsorbed alkaline phosphate conjugated anti-digoxygenin antibody was used in 1% BSA solution overnight at 4C. Reaction was developed in 1 mL total volume consisting of alkaline phosphate buffer, 6.6 µL nitro-blue tetrazolium chloride (NBT, Promega, Madison WI), and 3.3 µL 5-BRomo-4-chloro-3'-indolyphosphate p-toluidine salt (BCIP, Promega, Madison WI) at room temperature.

***dally* amplification:**

A 918 base pair region of *dally* was amplified for use as a species-specific *in situ* probe from *D. willistoni* cDNA using 5' TGTGCAGCTATTTCCTGTCG 3' and 3'TCGTTCAGTTTGCTGACCTG 5' primers generated with Primer3 v0.4.0 (Rozen and Skaletsky, 2000) in conjunction with FastA sequence data available at FlyBase (gene

symbol GK16744). PCR was conducted with a MJ Mini (BioRad, Hercules CA) thermocycler. Digoxygenin-labeled probes made with DIG RNA labeling kit (Roche, Branford CT).

Immunohistochemistry:

Immunoassay protocol was done as previously described (Pacquelet and Rorth, 2005). Ovary dissection and fixation were conducted as in RNA *in situ* hybridization, but without DMSO in the fixation mixture. Primary antibodies used were: rabbit anti-phosphorylated-Smad1/5/8 (1:3500, a gift from D. Vasiliauskas, S. Morton, T. Jessel, and E. Laufer), mouse anti-Broad core (25E9.D7; 1:100, DSHB), and sheep anti-GFP (AbD Serotec, 1:1250). Secondary antibodies used were: Alexa Fluor-488nm-conjugated goat anti-mouse, Alexa Fluor-568nm goat anti-rabbit, Alexa Fluor-488nm donkey anti-sheep (all 1:1250), and DAPI (1:5000).

Microscopy:

Egg chambers were imaged with a Leica DM2500 compound light microscope at 100, 200, or 400x and QCapture image capture software. Eggs for imaging via scanning electron microscopy were collected on agar plates and mounted on aluminum SEM stubs with double-sided carbon tape ≤30 minutes after oviposition. The stubs and eggshells were then immediately sputter coated with gold/palladium with a Denton Vacuum Desk II sputter coater before being imaged using a LEO 1450EP at high vacuum ($<1x10^{-5}$ torr). Captured images were rotated, cropped, and prepared using NIH ImageJ.

Quantification of BMP signaling:

Signaling was measured as the average intensity of P-Mad staining in dorsal views of late stage 10A egg chambers (Fig. 7 A). Images were imported into ImageJ and pixel intensities were measured by boxing subsets of follicle cells beginning at the midpoint of the anterior-most follicle cells (Fig. 7 B). In an effort to control for effects of the protocol on background and final staining intensity, immunohistochemistry protocols for these samples were conducted in parallel, and staining was carried out using common batches of primary and secondary antibody mixtures. The average of these plot profiles were normalized such that the highest intensity P-Mad staining, from the position of the center of the anterior most follicle cell, were equal to 1.00, with all subsequent values represented as a fraction of 1.00 relative to their intensity and plotted with standard error bars (Graph 1).

Quantification of changes in Broad patterning:

Broad (BR) patterns were quantified by comparing the average shape of the midline clearing of BR in dorsal views of early stage 10B egg chambers. The number of cells in which BR was not observed (green, Fig. 9 A) was counted beginning at the dorsal midline of the dorsal anterior and counting proceeding towards the posterior (along the white lines, Fig. 9 A). The average shape of the midline clearing of BR was calculated for each perturbation beginning with the row of cells directly overlying the dorsal midline and moving laterally in each direction. Since the midline is symmetrically distributed,

the values for one egg chamber were counted in both directions away from an imaginary central line of the dorsal-midline which resulted in the average shape of one half of the midline clearing. These averages were plotted such that the row of cells over the dorsal midline were at X=0, with standard error bars overlaid (Graph 2).

Quantification of operculum changes due to *dally* perturbations:

Images captured with SEM were imported to ImageJ and scales we calculated using built in tools in conjunction with scale information from the SEM. Then, length data were collected for zones 1, 2, and 3 of the operculum as well as for the length of the entire egg shell from the bottom of the micropyle's base to the posterior end of the aeropyle (Fig. 10 A, B). Data was collected, averages and standard error calculated from the raw data, which was then adjusted such that final values were percent differences from wild-type OreR control (Graph 3). Paired two sample (assuming unequal variances) *t*-tests were carried out on the raw data for comparison, differences with two-tailed $p < 0.05$ were considered to be significant and marked with an asterisk.

Results

dally expression pattern

The expression pattern of *dally* in *D. melanogaster* was previously described (Yakoby et al., 2008a). In *D. melanogaster dally* is expressed dynamically in the FCs. In *D. melanogaster dally* is not expressed during stage 9 (Fig. 4 A). Later, at stage 10A, *dally* is expressed at a high level in an anterior ring and at a lower level throughout the remainder of the follicle cells (Fig. 4 B). This pattern persisted through stage 10B (Fig. 4 C), when *dally* expression begun to clear from the dorsal anterior. After stage 10B *dally* expression was no longer detectable (Fig. 4 D). Similar patterns of *dally* were observed in *D. nebulosa* (Fig. 5 A) as well as *D. willistoni* (Fig. 5 B). In both these species *dally* is expressed in higher levels in the anterior-most ring of follicle cells and at a lower level throughout the FCs as in *D. melanogaster*.

dally expression is regulated by BMP signaling

High expression level of *dally,* (Fig. 6 A) in the anterior FCs overlap with the domain of high P-Mad expression (Fig. 6 B). Thus, we hypothesized that *dally* is a target of BMP signaling. To test this hypothesis, we ectopically expressed the BMP ligand Dpp in the posterior domain using E4-GAL4. This perturbation was sufficient to induce P-Mad expression in the posterior domain (Fig. 6 C). Interestingly, this was also sufficient to obtain high level of *dally* expression in this domain (Fig. 6 D). This was confirmed again through ectopic expression of the constitutively active form of the BMP receptor Tkv*

(Lecuit et al., 1996) using the same driver (Fig. 6 E). When Tkv* was ectopically expressed uniformly throughout the FCs with the CY2-GAL4 driver, high levels of *dally* expression were observed uniformly throughout the follicle cells except where it was repressed in the dorsal domain (Fig. 6 F). Overexpression of the BMP inhibitor *dad* throughout the FCs lead to no observable *dally* expression (Fig. 6 G). These results suggest that *dally* is a target of BMP signaling.

Dally is necessary for BMP signaling

In wild-type OreR, P-Mad is detected in 2-3 rows of anterior FCs (Graph 1, blue line, Fig. 8 A) (Yakoby et al., 2008b; Niepielko et al., 2011). Uniform overexpression of Dally resulted in an expansion of the P-Mad gradient distal from the anterior (Graph 1, black line, Fig. 8 B). The depletion of *dally* throughout the FCs using the GR1-GAL4 driver restricted the domain of P-Mad expression to the anterior (Graph 1, red line, Fig. 8 C). In this perturbation ectopic P-Mad was also detected in the posterior. Similar results were obtained when *dally* was depleted with the shDally line in the same domain (results not shown). To determine whether *dally* was regulating BMP signaling in a cell autonomous manner, we induced mitotic clones of loss of function *dally* using the FLP/FRT recombinase system. In these clones, P-Mad was lost cell autonomously in anterior follicle cells (Fig. 8 D). Thus, *dally*, is not only a downstream target of BMP signaling but is also required for BMP signaling (Fig. 8 E).

Perturbations of *dally* modify tissue patterning

Using BR expression as a spatial marker, I quantified changes in BR expression as an indicator for changes in tissue patterning resulting from perturbations of *dally* (Fig. 9). In lateral-anterior FCs of the wild-type OreR, BR was cleared an average of 3 cells toward the posterior (Graph 2, blue line). Uniform depletion of *dally* resulted in an approximately one cell shift of BR towards the anterior (Graph 2, red line). Overexpression of *dally* in the same uniform domain resulted in a shift of BR patterning towards the posterior (Graph 2, black line).

Eggshell morphology is disrupted in perturbations of *dally*

Depletion of *dally* in the stretch cells and anterior-most FCs with Dad-GAL4 (Pope and Yakoby, unpublished) driving Dally RNAi resulted in a significant decrease of over 20% in the length of the operculum relative to OreR in the length of zone one of the operculum. It also resulted in significant increases of 30% and 10% in the lengths of zones two and three respectively (Graph 3 A). Overexpression of *dally* in the same domain resulted in significant increases of over 10% in zone two and over 10% in zone 3, but did not have an effect on zone 1 (Graph 3 B). Asterisks mark columns where raw data was significantly different ($p<0.05$) from wild-type OreR (Graph 3).

Discussion

Glypicans have previously been shown to interact with ligands from the Wingless, Hedgehog, and BMP signaling pathways in the wing imaginal discs (Han et al., 2004; Lin, 2004). Additionally, it has even been suggested that the movement of most or all signaling molecules is mediated by HSPGs (Crickmore and Mann, 2007). Due to their involvement in processes that are critical for cells and tissue development, there is much to gain by sequencing the 'heparanome', the long chains of heparan sulfate sequences which are attached to the protein cores of these molecules (Turnbull et al., 2001). These molecules then, present an interesting avenue for research into cell signaling and the processes beyond simple, unimpeded or altered diffusion of morphogen gradients. Specifically, differential expression of the glypican Dally has been shown to help in regulating the diffusion of the BMP ligand Dpp, and consequently shaping the domain of activated BMP signaling in the *Drosophila* haltere, an organ involved in flight, and is also used as a model system for BMP signaling (Crickmore and Mann, 2007).

In the haltere, *dally* is expressed in high levels in the regions directly adjacent to either side of the anterior-posterior organizer (Crickmore and Mann, 2007). This domain is responsible for the bulk production of Dpp. This domain is analogous to the anterior-most FCs and stretch cells of *Drosophila* oogenesis (Fig. 2 B) (Twombly et al., 1996). Just as in the haltere, *dally* expression during oogenesis is higher nearest the source of the ligand Dpp (Fig. 4 & 5). Remarkably, this pattern is conserved over 36

million years (+ or – 4) of *Drosophila* evolution , which suggests a functional role for Dally during FCs development (Fig. 5) (Pitnick et al., 1995; Russo et al., 1995). However, unlike the haltere, where the experimental data show that *dally* is repressed by BMP signaling, in the FCs we show that *dally* expression is positively regulated by BMP signaling in the FCs (Fig. 6). Here we show that *dally* expression follows ectopic activation of BMP signaling (Fig. 6 D). Consistent with this hypothesis, repression of BMP signaling abolishes *dally* expression from the FCs (Fig. 6 G).

The uniform, basal level of *dally* expression may be dependent upon different signaling pathways, possibly Ecdyson, Hedgehog, or Wingless signaling, which have previously been shown to induce *dally* expression in other tissues (Crickmore and Mann, 2006). The dorsal clearing of *dally* in overexpression of Tkv* throughout the FCs may be dependent upon other signaling pathways which are not inhibited by BMP signaling, possibly EGFR signaling, as other pathways have been implicated in the regulation of *dally* (Cadigan and Nusse, 1997; Baeg et al., 2001).

The mechanism by which Dally affects the Dpp gradient has previously been described as stabilizing Dpp on the cell surface during wing development .However, this interaction with Dpp has also been shown not to depend entirely on heparan sulfate modification (Kirkpatrick et al., 2006). Because of this, it is believed that the protein core of Dally may contribute much of its growth factor binding properties. This is consistent with experimental data which showed that BMP4, the vertebrate homolog of Dpp is capable of interacting with both Dally's protein core as well as its heparan sulfate chains (Kirkpatrick et al., 2006). Based upon these observations, as well as our own P-

Mad staining intensity data (Graph 1), we propose that Dally modulates the diffusion of Dpp away from the Dpp-secreting cells (Graph 1), and that over or under expression of *dally* results in an increase or decrease, respectively, in the length of the Dpp gradient (Fig. 8 E).

Interestingly, it appears that Dpp is capable of diffusing over cells null for *dally*. In mosaic tissue, we detect P-Mad staining in cells that are posterior to cells with *dally* loss of function (Fig. 8 D). This would likely result in an increase in free Dpp ligand, however in a mosaic tissue, we do not observe ectopic P-Mad beyond the established domain of BMP signaling and high level *dally* expression. This, in conjunction with the cell-autonomous loss of P-Mad in cells null for *dally* indicates that high levels of Dally must be required for the perception of the Dpp gradient and BMP signaling, suggesting a role for high levels of Dally as a necessary co-receptor (Fig. 7 E) (Fujise et al., 2003).

If BMP signaling is indeed affected by perturbations of *dally* (Jackson et al., 1997; Fujise et al., 2003; Belenkaya et al., 2004), then tissue patterning reliant upon positional information from BMP signaling must be effected. Since P-Mad represses BR during oogenesis (Yakoby et al., 2008b), if perturbations of *dally* are affecting BMP signaling, we expect to observe changes in the BR pattern. Indeed, we found this to be the case (Graph 2). Specifically, we observe that the wild-type expression of BR is shifted to the anterior in loss-of-function perturbations, consistent with a decrease in BMP signaling (Fig. 9 C) (Lembong et al., 2009). Conversely, in overexpression of *dally* we observe a shift in BR away from the posterior (Fig. 9 D). This repression of BR in the anterior of uniform overexpression of *dally* is longer than the observed changes in P-Mad intensity,

which indicates that signaling levels may actually be increased, however, these levels are below our detection abilities (Fig. 9 D, Graph 1).

Consistent with changes in patterning through modifications in BMP signaling, we observe that the operculum, one of the three dimensional structures of the *Drosophila* eggshell that is sensitive to changes in the levels of BMP signaling, is disrupted in *dally* perturbations (Graph 3). The wild-type operculum (Fig. 10 B) is composed of three zones (Shravage et al., 2007). Zone one of the operculum derives from the anterior-most follicle cells at stage 10, while the second and third zones are laid down by FCs further away from the anterior and between the high level BR patches, respectively (Fig. 3 B).

In loss-of-function perturbation of *dally* in the anterior FCs and stretch cells with Dad-GAL4 (Graph 3 A); the population of cells which overlaps the Dpp source derive the formation of zone 1 of the operculum (Fig. 3 B), is significantly reduced. At the same time, zones two and three are significantly increased in length (Graph 3 A). It was proposed that BMP signaling is critical to the formation of all zones of the operculum (Shravage et al., 2007). The reduction of *dally* in Zone 1 will reduce signaling in this zone, while providing more free Dpp to zones 2 and 3, consequently increasing their sizes.

In overexpression of *dally* (Graph 3 B), the first zone of the operculum is not significantly different in length from the wild-type OreR, while the second and third zones are both significantly expanded. This similar phenotype to loss-of-function can be explained via the expansion of the Dpp gradient, as evident in the extended P-Mad gradient (Graph 1, Fig. 8 B) and the shift in BR patterning (Graph 2, Fig. 9 D). If Dally is

capable of expanding the Dpp gradient by affecting its diffusion as was previously suggested (Jackson et al., 1997; Dejima et al., 2011), this perturbation will increase the free-ligand available to zones 2 and 3. Such an increase in Dpp would increase signaling and consequently, the lengths of zones 2 and 3.

Perturbations of *dally* may affect other signaling pathways in *Drosophila* oogenesis besides BMP signaling. The ectopic P-Mad observed in uniform depletion of *dally* may be indicative of a reduction in EGFR signaling which is needed to repress BMP signaling in the posterior. Additionally, while changes in the width of the operculum have not been observed, effects on the DAs, including merged or fused DAs have been observed in depletion of *dally*. This phenotype is also associated with changes in the levels of EGFR signaling (Wang et al., 2008; Pizette et al., 2009) which controls the gap between the DAs. This is an interesting possibility, as it could mean that Dally coordinates tissue patterning along two axes, through effects on EGFR signaling.

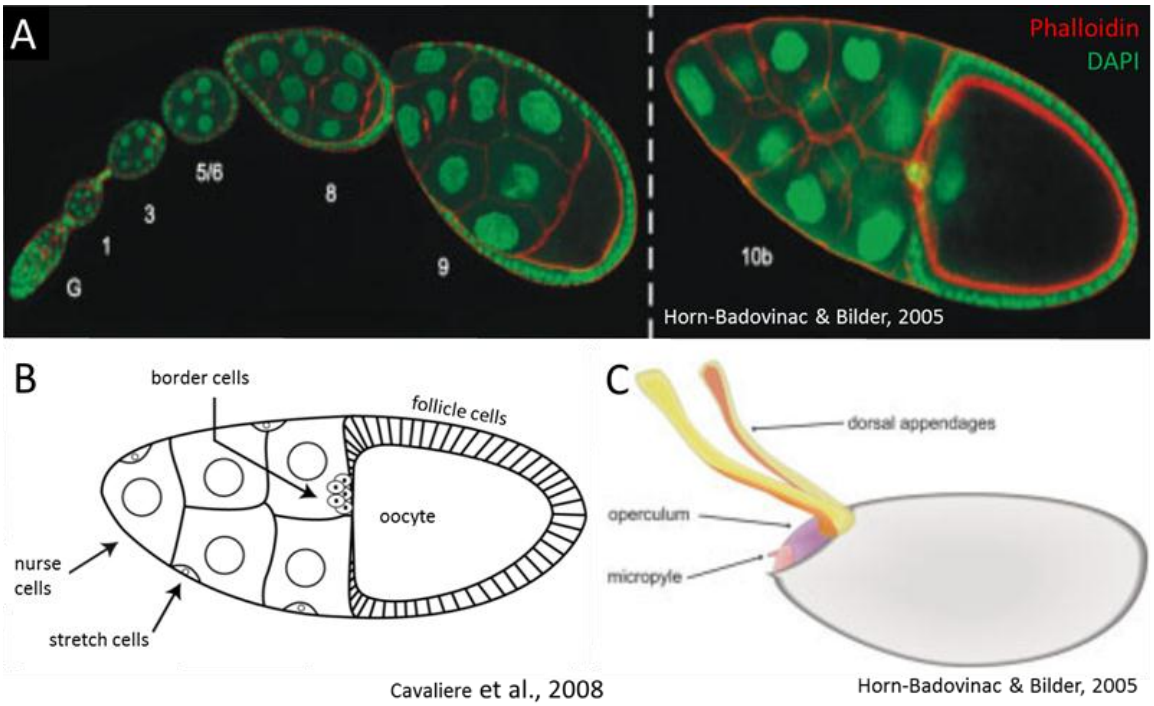

FIGURE 1: *Drosophila melanogaster* oogenesis
(A) Egg chambers at stages 1 through 10B of *D. melanogaster* oogenesis (anterior is to the left, nuclei marked with DAPI, green, membranes marked with phalloidin, red).
(B) Cartoon of stage 10 egg chamber (lateral view). Oocyte is surrounded by follicle cells (FCs). Nurse cells toward the anterior, which supply the oocyte with nutrients, are themselves surrounded by the epithelial stretch cells.
(C) Cartoon of mature eggshell showing three dimensional structures. The dorsal appendages are cylindrical structures on dorsal anterior, operculum is anterior structure larva will exit the eggshell through. The cone shaped micropyle allows for sperm entry during fertilization.

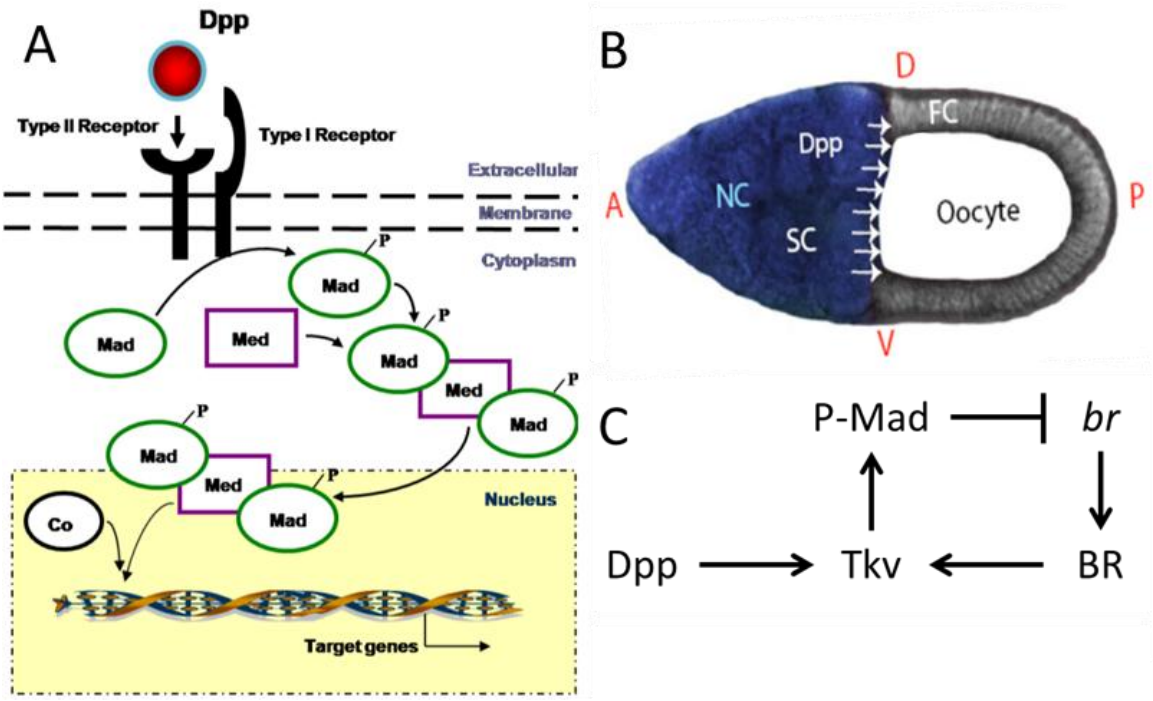

FIGURE 2: Bone morphogenetic protein (BMP) signaling in *D. melanogaster* oogenesis

(A) Diagram of BMP signaling internalization. Dpp binds the Type I, Type II receptor complex and is internalized, resulting in the phosphorylation of Mad (P-Mad), which together with Medea (Med) and other mediators acts as a transcription factor.

(B) Colored egg chamber. Dpp gradient from left to right. Lateral view, anterior towards the left, dorsal towards the top. Additional information can be found in Fig. 1 B.

(C) Summary of BMP signaling network. Dpp binds Tkv, resulting in P-Mad, which represses *br.*

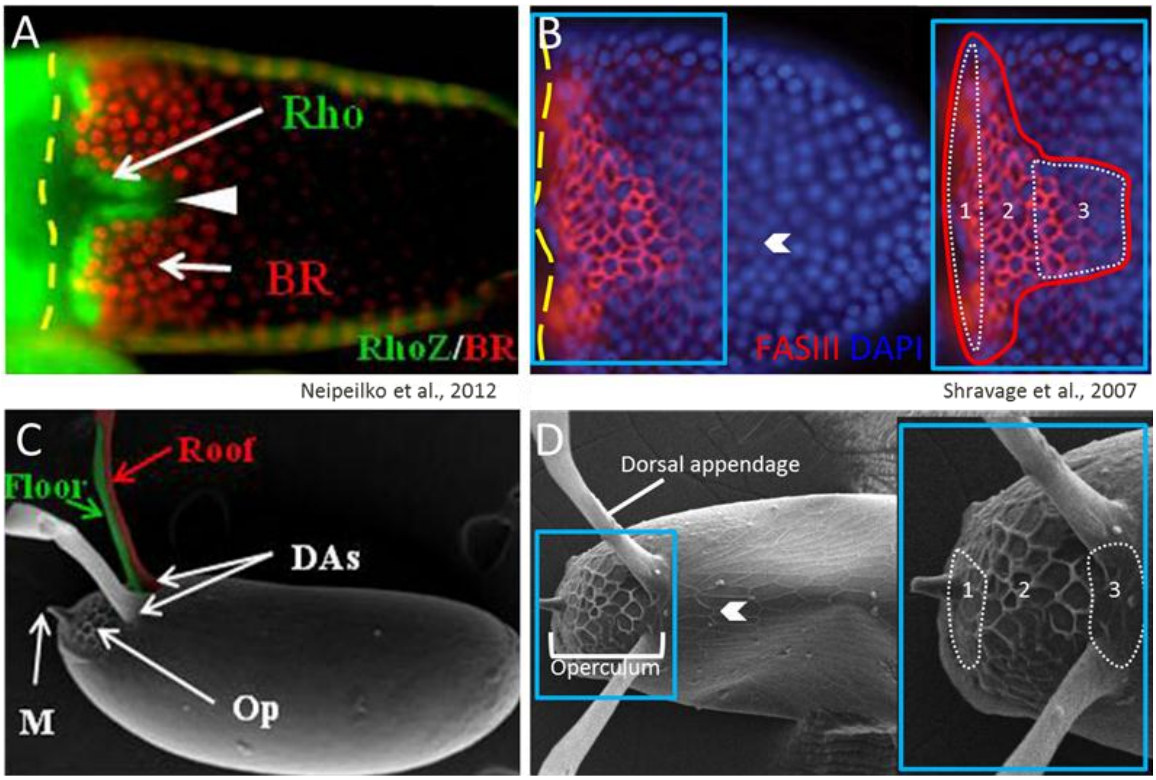

FIGURE 3: Patterning the *D. melanogaster* eggshell
(A) Broad (BR) expressing cells (red) give rise to roof of the dorsal appendages (C), Rhomboid (Rho) expressing cells (green) give rise to floor of the dorsal appendages (C).
(B) Fasciclin III (FAS III) expressing cells give rise to the operculum (zones outlined in white dotted lines, inset).
(D) SEM micrograph of *Drosophila melanogaster* eggshell, operculum magnified in inset (zones of operculum outlines in white dotted lines).

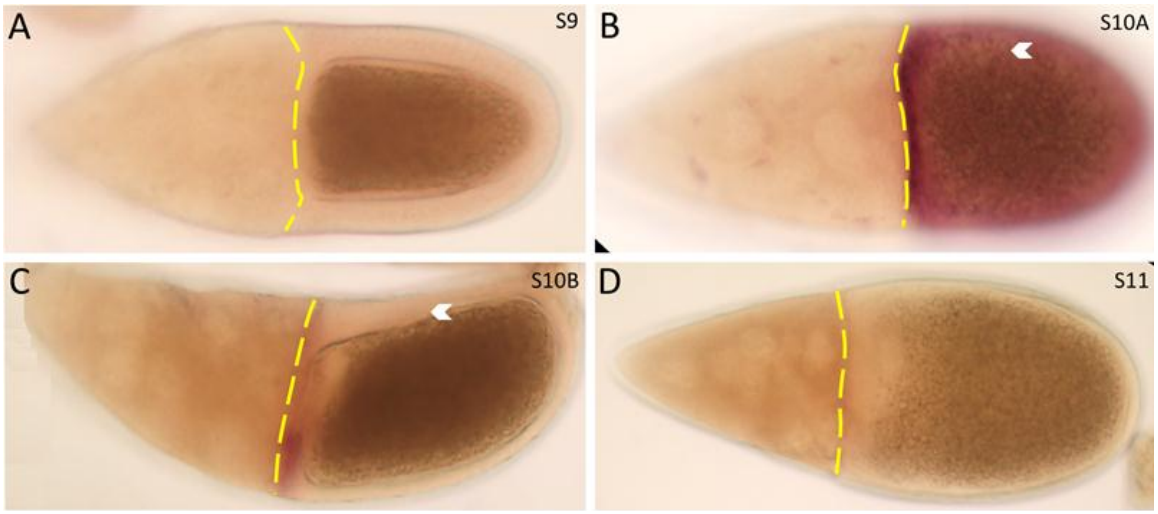

FIGURE 4: *dally* expression dynamics in *D. melanogaster*
(A) *in situ* hybridization for *dally,* stage 9 wild-type *Drosophila melanogaster* egg chamber.
(B) Stage 10A egg chamber. *dally* expression at a higher level in the anterior most FCs (anterior marked with yellow hashed line), lower level *dally* throughout the FCs.
(C) Stage 10B egg chamber showing dorsal clearing in high level *dally* expression (dorsal marked with white chevron).
(D) Stage 11 egg chamber showing lack of *dally* expression.
Lateral views of all egg chambers.

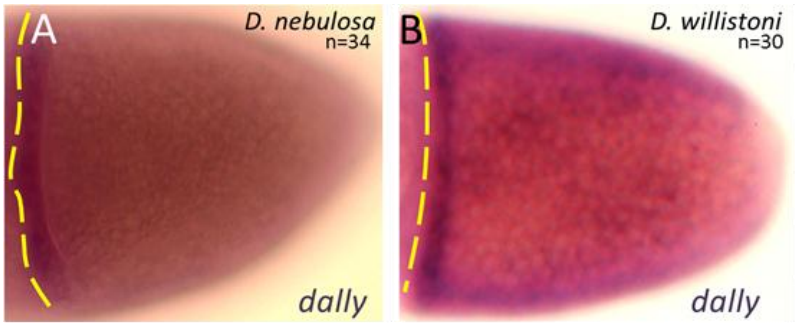

FIGURE 5: *dally* expression in other species
(A) *in situ* hybridization for dally in *Drosophila nebulosa*. Similar dally pattern to *D. melanogaster*.
(B) *in situ* for *dally* in *Drosophila willistoni. dally* expression pattern similar to *D. melanogaster.*
Lateral views of all egg chambers, anterior marked with hashed yellow line, dorsal towards the top. n represents number of stage 10 egg chambers with this pattern.

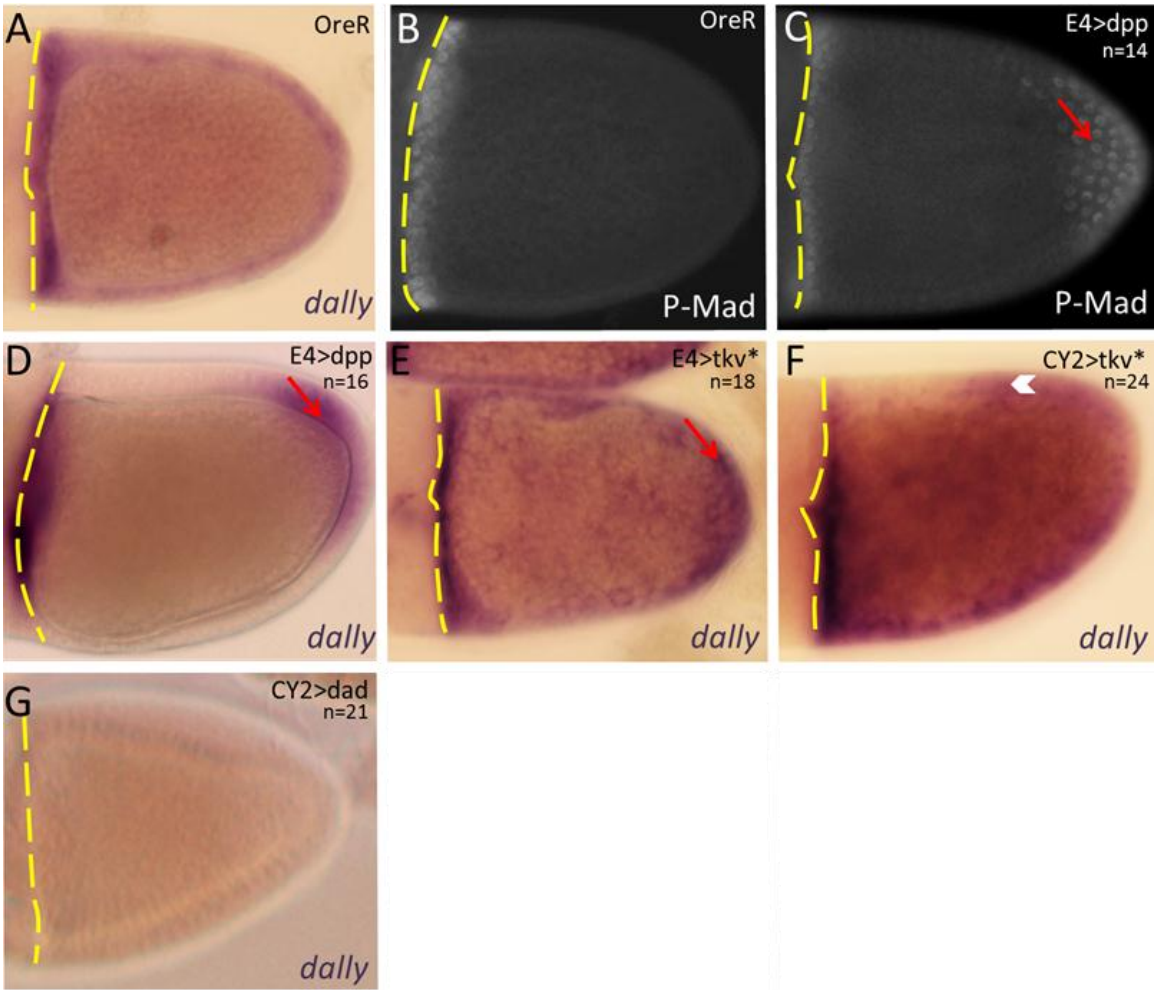

FIGURE 6: *dally expression* is regulated by BMP signaling
(A) Wild-type high level *dally* expression overlaps with the anterior (marked with yellow hashed line) high level of P-Mad (B).
(C) Ectopic expression of Dpp in the posterior domain induced P-Mad (red arrow) and it induced ectopic high level *dally* expression in this domain (red arrow).
(E) High level of *dally* in ectopic expression of an activated form of a BMP receptor Tkv (Tkv*) in the posterior (red arrow).
(F) Uniform expression of Tkv* results in uniform high level *dally* throughout the FCs except for the dorsal domain (marked with white chevron).
(G) Uniform expression of the BMP inhibitor Daughters-against-Dpp (Dad) represses *dally* expression throughout the FCs.

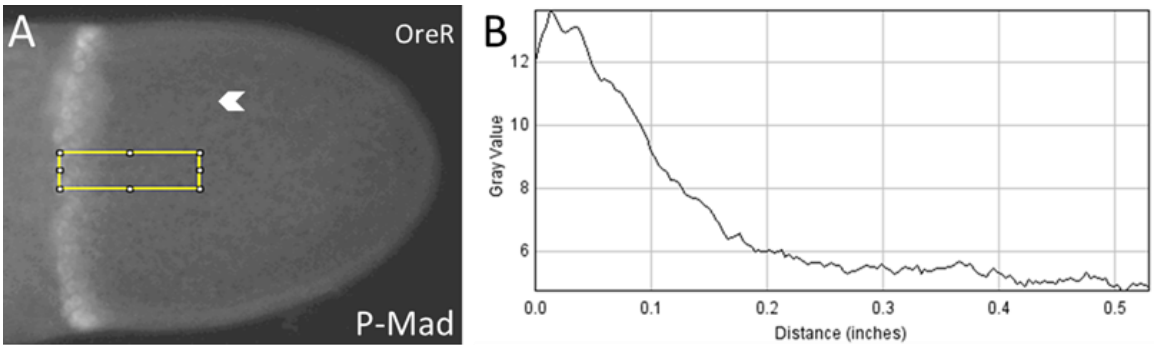

FIGURE 7: Quantification of P-Mad intensity
(A) Dorsal view of late stage 10A egg chamber, stained for P-Mad. Average staining intensities from yellow boxes were plotted over distance toward posterior. Boxes were placed along the dorsal anterior (dorsal marked with white chevron) as stated in Quantification of P-Mad Intensities, Materials & Methods.
(B) Plot profile from sample yellow box in (A), calculated in ImageJ. Average P-Mad intensity from all egg chambers plotted in Graph 1.

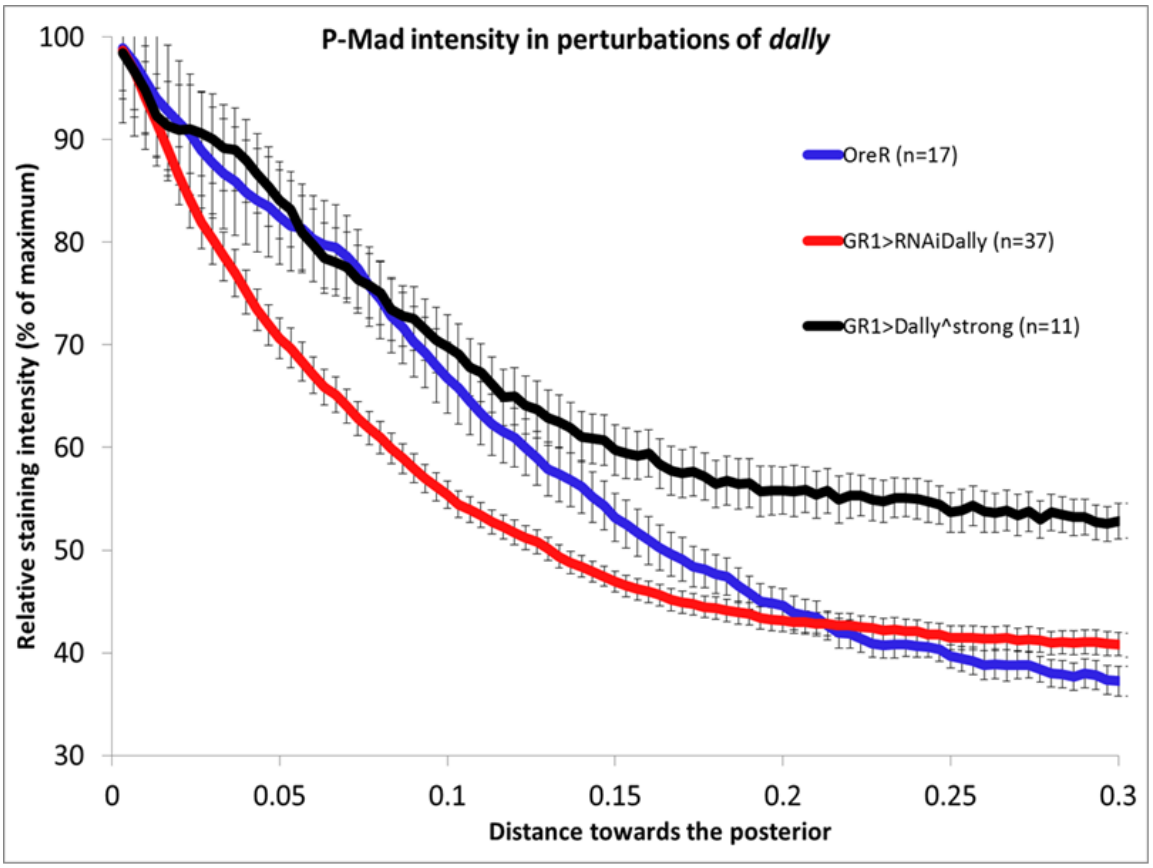

Graph 1:
Relative intensity of P-Mad staining in ectopic over and underexpression of *dally*. Wild-type P-Mad (blue line) declines slowly from anterior to posterior. Overexpression of *dally* (black line) results in P-Mad persisting further into the posterior domain. Depletion of *dally* with RNAi (red line) results in a sharper decline in P-Mad intensity than wild-type. Error bars represent standard error, distance and intensities measured in arbitrary units with ImageJ. n values represent numbers of plot profiles averaged for each treatment.

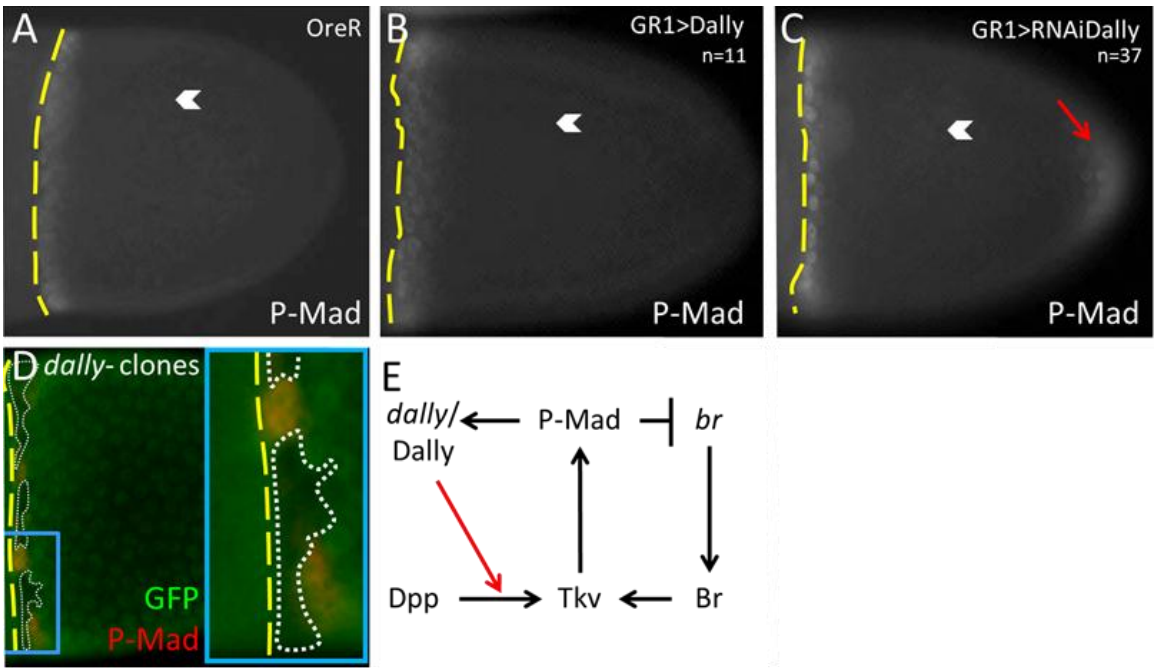

FIGURE 8: Dally is required for BMP signaling
(A) Wild-type P-Mad staining extends 2-3 cell rows from the anterior (yellow hashed line).
(B) Uniform overexpression of *dally* expands the P-Mad gradient to 3-4 cell rows from the anterior.
(C) Uniform depletion of *dally* results in constricted P-Mad gradient, ectopic P-Mad observed in posterior (red arrow).
(D) Mosaic tissue, in cells null for *dally* (marked with lack of GFP and white dotted line, magnified in inset) P-Mad (red) is lost cell-autonomously.
(E) Summary of BMP signaling including *dally* as a downstream target and a role for Dally as a required component.

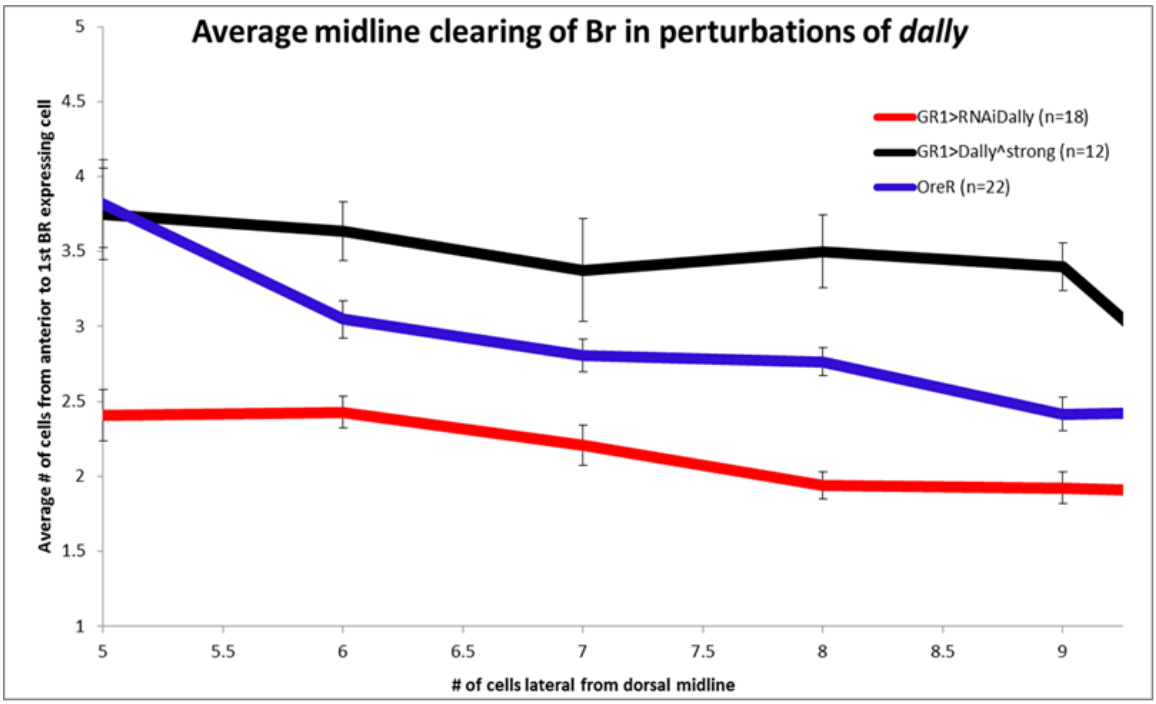

Graph 2:

Wild-type midline clearing (blue line) of BR in the anterior domain in 5 to 9 cells laterally to the dorsal-midline is approximately 3 cell rows deep. Depletion of *dally* (red line) results in a shift of BR towards the anterior. Overexpression (black line) results in a shift of BR toward the posterior. Error bars represent standard error.

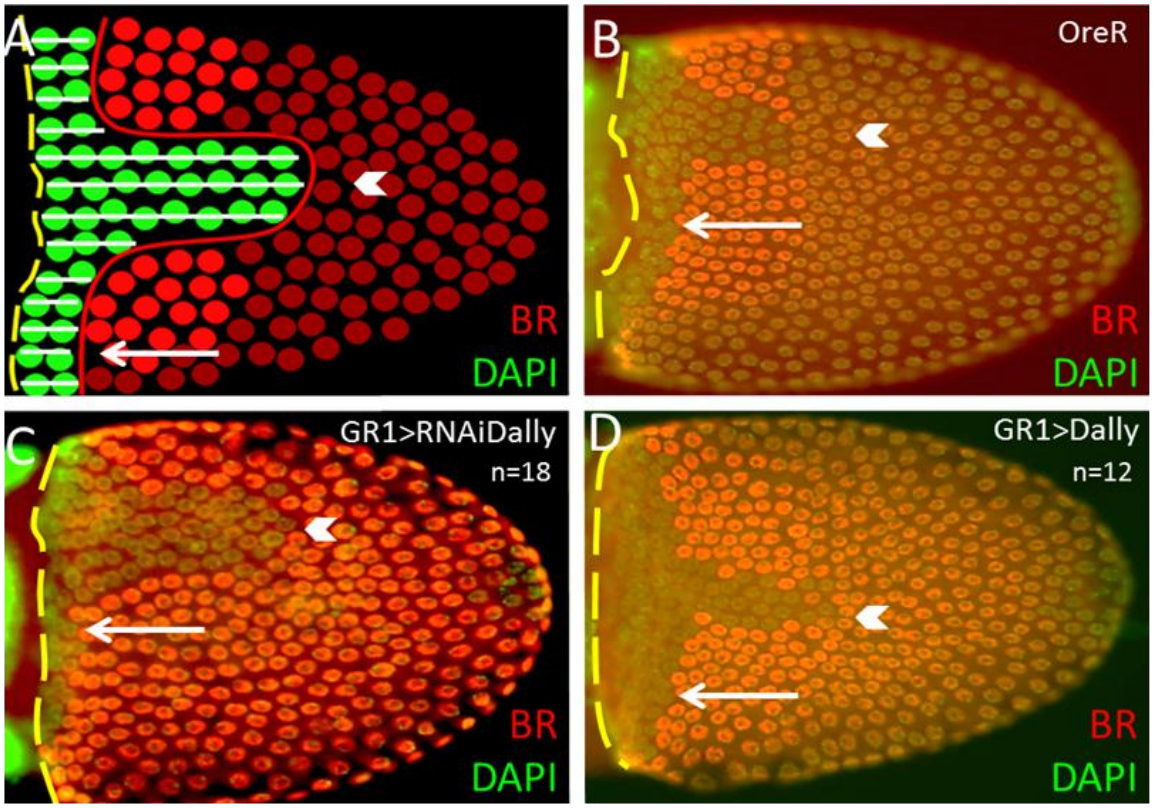

FIGURE 9: Perturbations of *dally* modify tissue patterning
(A) Schematic of BR (red) expressing egg chamber showing midline clearing (green). Cells counted from anterior along white lines to determine average number of cell rows in the clearing; which is plotted in Graph 2. Dorsal midline marked with white chevron, anterior marked with white hashed line.
(B) Wild-type midline clearing in BR approximately 3 cell rows deep in lateral anterior FCs (green, marked with white arrow)
(C) Uniform depletion of *dally* leads to an anterior shift in BR patterning (marked with white arrow).
(D) Uniform overexpression of *dally* results in a posterior shift in BR patterning (marked with white arrow).

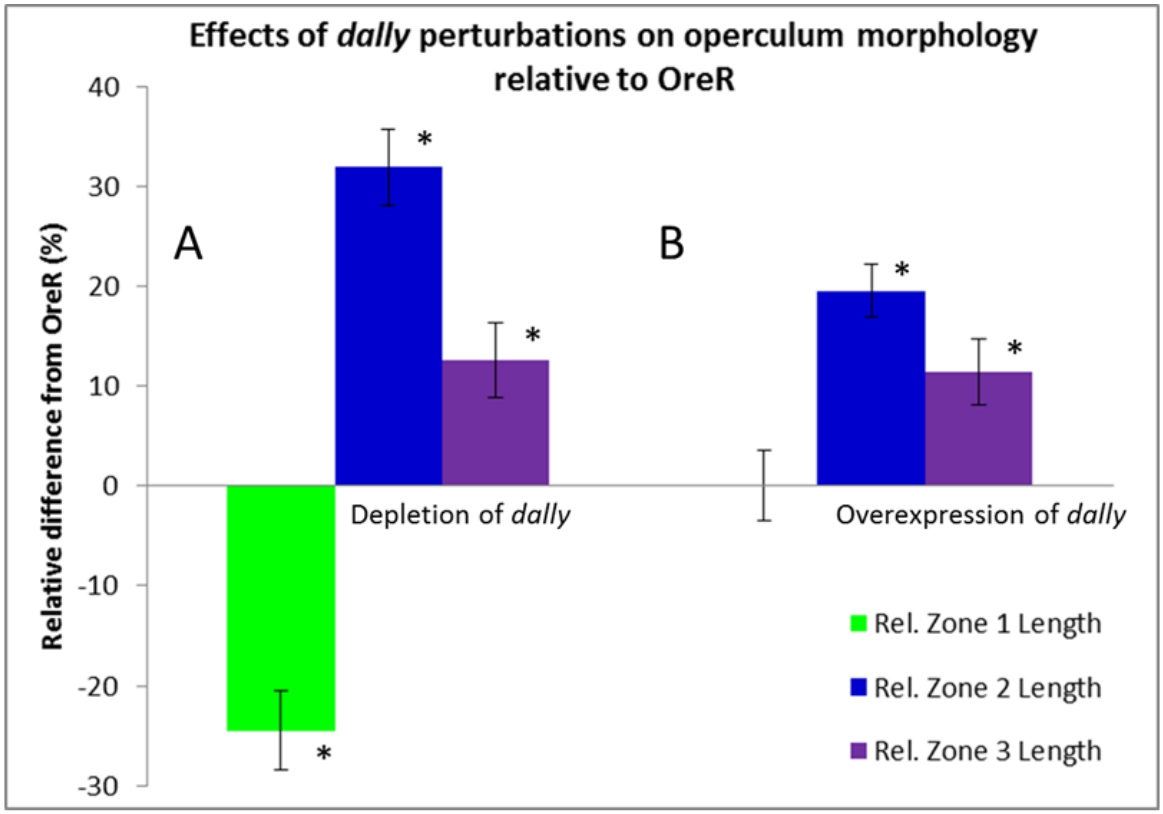

Graph 3:
(A) Depletion of *dally* with Dad-GAL4 results in significant decrease in length of zone 1 (green) relative to overall eggshell length when compared to wild-type OreR. Lengths of zones 2 (blue) and 3 (purple) relative to entire eggshell are significantly increased.
(B) Overexpression of *dally* in the same domain results in no effect on zone 1 length. Zones 2 and 3 are significantly increased in length.
Error bars represent standard error, asterisks represent significant differences in raw data averages when compared to OreR ($p<0.05$).

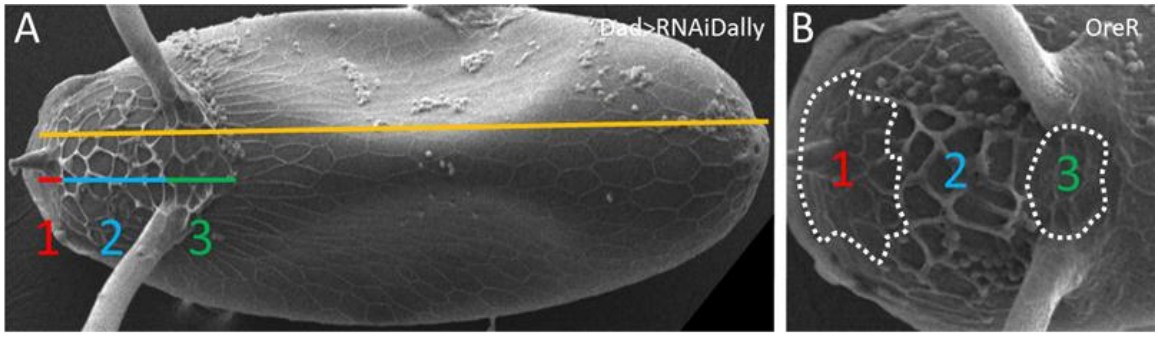

FIGURE 10: Perturbations of *dally* affect eggshell morphology
(A) SEM micrograph of *D. melanogaster* eggshell. Length of each operculum zone (red, blue, green lines) calculated relative to overall length of the eggshell (orange line); plotted in Graph 3.
(B) Operculum shown magnified. Zones 1 and 3 outlined with white dotted line.

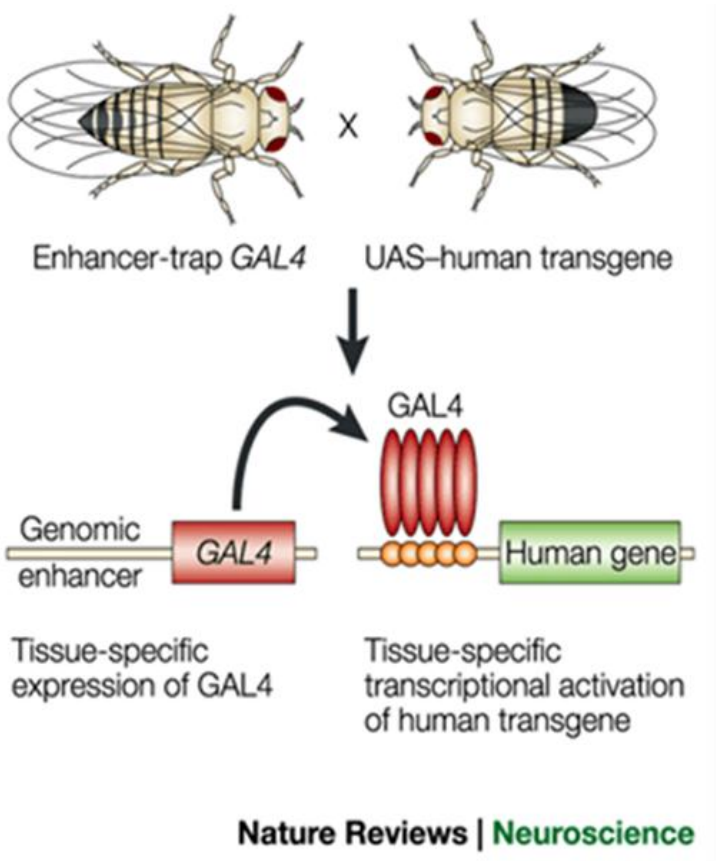

FIGURE 11: The GAL4/UAS system for targeted gene expression
Diagram of GAL4/UAS system used for targeted expression of genes or constructs. A parent fly which produces the yeast transcription factor GAL4 is crossed to a parent fly which contains upstream activating sequence (UAS) to a gene or construct of interest. Consequently, offspring ectopically express the UAS-gene or UAS-construct in the pattern of the GAL4 driver.

References

Akiyama, T., Kamimura, K., Firkus, C., Takeo, S., Shimmi, O. and Nakato, H. (2008) 'Dally regulates Dpp morphogen gradient formation by stabilizing Dpp on the cell surface', *Dev Biol* 313(1): 408-19.

Baeg, G. H., Lin, X., Khare, N., Baumgartner, S. and Perrimon, N. (2001) 'Heparan sulfate proteoglycans are critical for the organization of the extracellular distribution of Wingless', *Development* 128(1): 87-94.

Baker, J. C. and Harland, R. M. (1997) 'From receptor to nucleus: the Smad pathway', *Curr Opin Genet Dev* 7(4): 467-73.

Belenkaya, T. Y., Han, C., Yan, D., Opoka, R. J., Khodoun, M., Liu, H. and Lin, X. (2004) 'Drosophila Dpp morphogen movement is independent of dynamin-mediated endocytosis but regulated by the glypican members of heparan sulfate proteoglycans', *Cell* 119(2): 231-44.

Berg, C. A. (2005) 'The Drosophila shell game: patterning genes and morphological change', *Trends Genet* 21(6): 346-55.

Berg, C. A. (2008) 'Tube formation in Drosophila egg chambers', *Tissue Eng Part A* 14(9): 1479-88.

Blair, S. S. (2005) 'Cell signaling: wingless and glypicans together again', *Curr Biol* 15(3): R92-4.

Cadigan, K. M. and Nusse, R. (1997) 'Wnt signaling: a common theme in animal development', *Genes Dev* 11(24): 3286-305.

Crickmore, M. A. and Mann, R. S. (2006) 'Hox control of organ size by regulation of morphogen production and mobility', *Science* 313(5783): 63-8.

Crickmore, M. A. and Mann, R. S. (2007) 'Hox control of morphogen mobility and organ development through regulation of glypican expression', *Development* 134(2): 327-34.

Dejima, K., Kanai, M. I., Akiyama, T., Levings, D. C. and Nakato, H. (2011) 'Novel contact-dependent bone morphogenetic protein (BMP) signaling mediated by heparan sulfate proteoglycans', *J Biol Chem* 286(19): 17103-11.

Ding, K., Lopez-Burks, M., Sanchez-Duran, J. A., Korc, M. and Lander, A. D. (2005) 'Growth factor-induced shedding of syndecan-1 confers glypican-1 dependence on mitogenic responses of cancer cells', *J Cell Biol* 171(4): 729-38.

Dobens, L. L. and Raftery, L. A. (2000) 'Integration of epithelial patterning and morphogenesis in Drosophila ovarian follicle cells', *Dev Dyn* 218(1): 80-93.

Duffy, J. B. (2002) 'GAL4 system in Drosophila: a fly geneticist's Swiss army knife', *Genesis* 34(1-2): 1-15.

Edidin, M., Kuo, S. C. and Sheetz, M. P. (1991) 'Lateral movements of membrane glycoproteins restricted by dynamic cytoplasmic barriers', *Science* 254(5036): 1379-82.

Esko, J. D. and Zhang, L. (1996) 'Influence of core protein sequence on glycosaminoglycan assembly', *Curr Opin Struct Biol* 6(5): 663-70.

Eugster, C., Panakova, D., Mahmoud, A. and Eaton, S. (2007) 'Lipoprotein-heparan sulfate interactions in the Hh pathway', *Dev Cell* 13(1): 57-71.

Fujise, M., Takeo, S., Kamimura, K., Matsuo, T., Aigaki, T., Izumi, S. and Nakato, H. (2003) 'Dally regulates Dpp morphogen gradient formation in the Drosophila wing', *Development* 130(8): 1515-22.

Han, C., Belenkaya, T. Y., Wang, B. and Lin, X. (2004) 'Drosophila glypicans control the cell-to-cell movement of Hedgehog by a dynamin-independent process', *Development* 131(3): 601-11.

Horne-Badovinac, S. and Bilder, D. (2005) 'Mass transit: epithelial morphogenesis in the Drosophila egg chamber', *Dev Dyn* 232(3): 559-74.

Jackson, S. M., Nakato, H., Sugiura, M., Jannuzi, A., Oakes, R., Kaluza, V., Golden, C. and Selleck, S. B. (1997) 'dally, a Drosophila glypican, controls cellular responses to the TGF-beta-related morphogen, Dpp', *Development* 124(20): 4113-20.

Kirkpatrick, C. A., Knox, S. M., Staatz, W. D., Fox, B., Lercher, D. M. and Selleck, S. B. (2006) 'The function of a Drosophila glypican does not depend entirely on heparan sulfate modification', *Dev Biol* 300(2): 570-82.

Kooyman, D. L., Byrne, G. W., McClellan, S., Nielsen, D., Tone, M., Waldmann, H., Coffman, T. M., McCurry, K. R., Platt, J. L. and Logan, J. S. (1995) 'In vivo transfer of GPI-linked complement restriction factors from erythrocytes to the endothelium', *Science* 269(5220): 89-92.

Lander, A. D., Stipp, C. S. and Ivins, J. K. (1996) 'The glypican family of heparan sulfate proteoglycans: major cell-surface proteoglycans of the developing nervous system', *Perspect Dev Neurobiol* 3(4): 347-58.

Lecuit, T., Brook, W. J., Ng, M., Calleja, M., Sun, H. and Cohen, S. M. (1996) 'Two distinct mechanisms for long-range patterning by Decapentaplegic in the Drosophila wing', *Nature* 381(6581): 387.

Lembong, J., Yakoby, N. and Shvartsman, S. Y. (2009) 'Pattern formation by dynamically interacting network motifs', *Proc Natl Acad Sci U S A* 106(9): 3213.

Lin, X. (2004) 'Functions of heparan sulfate proteoglycans in cell signaling during development', *Development* 131(24): 6009-21.

Massague, J. and Gomis, R. R. (2006) 'The logic of TGFbeta signaling', *FEBS Lett* 580(12): 2811-20.

Matsuda, K., Maruyama, H., Guo, F., Kleeff, J., Itakura, J., Matsumoto, Y., Lander, A. D. and Korc, M. (2001) 'Glypican-1 is overexpressed in human breast cancer and modulates the mitogenic effects of multiple heparin-binding growth factors in breast cancer cells', *Cancer Res* 61(14): 5562-9.

Muqit, M. M. and Feany, M. B. (2002) 'Modelling neurodegenerative diseases in Drosophila: a fruitful approach?', *Nat Rev Neurosci* 3(3): 237-43.

Neuman-Silberberg, F. S. and Schupbach, T. (1994) 'Dorsoventral axis formation in Drosophila depends on the correct dosage of the gene gurken', *Development* 120(9): 2457-63.

Niepielko, M. G., Hernaiz-Hernandez, Y. and Yakoby, N. (2011) 'BMP signaling dynamics in the follicle cells of multiple Drosophila species', *Dev Biol* 354(1): 151-9.

Pacquelet, A. and Rorth, P. (2005) 'Regulatory mechanisms required for DE-cadherin function in cell migration and other types of adhesion', *J Cell Biol* 170(5): 803-12.

Padgett, R. W., St Johnston, R. D. and Gelbart, W. M. (1987) 'A transcript from a Drosophila pattern gene predicts a protein homologous to the transforming growth factor-beta family', *Nature* 325(6099): 81-4.

Parker, L., Stathakis, D. G. and Arora, K. (2004) 'Regulation of BMP and activin signaling in Drosophila', *Prog Mol Subcell Biol* 34: 73-101.

Pitnick, S., Markow, T. A. and Spicer, G. S. (1995) 'Delayed male maturity is a cost of producing large sperm in Drosophila', *Proc Natl Acad Sci U S A* 92(23): 10614-8.

Pizette, S., Rabouille, C., Cohen, S. M. and Therond, P. (2009) 'Glycosphingolipids control the extracellular gradient of the Drosophila EGFR ligand Gurken', *Development* 136(4): 551-61.

Raftery, L. A. and Umulis, D. M. (2012) 'Regulation of BMP activity and range in Drosophila wing development', *Curr Opin Cell Biol* 24(2): 158-65.

Rozen, S. and Skaletsky, H. (2000) 'Primer3 on the WWW for general users and for biologist programmers', *Methods Mol Biol* 132: 365-86.

Ruohola-Baker, H., Grell, E., Chou, T. B., Baker, D., Jan, L. Y. and Jan, Y. N. (1993) 'Spatially localized rhomboid is required for establishment of the dorsal-ventral axis in Drosophila oogenesis', *Cell* 73(5): 953-65.

Russo, C. A., Takezaki, N. and Nei, M. (1995) 'Molecular phylogeny and divergence times of drosophilid species', *Mol Biol Evol* 12(3): 391-404.

Salmivirta, M., Lidholt, K. and Lindahl, U. (1996) 'Heparan sulfate: a piece of information', *FASEB J* 10(11): 1270-9.

Shravage, B. V., Altmann, G., Technau, M. and Roth, S. (2007) 'The role of Dpp and its inhibitors during eggshell patterning in Drosophila', *Development (Cambridge, England)* 134(12): 2261.

Spradling, A. C. (1993) *Developmental genetics of oogenesis. In: The Development of Drosophila melanogaster*: Plainview: Cold Spring Harbor Laboratory Press.

St Johnston, D. (2002) 'The art and design of genetic screens: Drosophila melanogaster', *Nat Rev Genet* 3(3): 176-88.

Takeo, S., Akiyama, T., Firkus, C., Aigaki, T. and Nakato, H. (2005) 'Expression of a secreted form of Dally, a Drosophila glypican, induces overgrowth phenotype by affecting action range of Hedgehog', *Dev Biol* 284(1): 204-18.

Tsuneizumi, K., Nakayama, T., Kamoshida, Y., Kornberg, T. B., Christian, J. L. and Tabata, T. (1997) 'Daughters against dpp modulates dpp organizing activity in Drosophila wing development', *Nature* 389(6651): 627.

Turnbull, J., Powell, A. and Guimond, S. (2001) 'Heparan sulfate: decoding a dynamic multifunctional cell regulator', *Trends Cell Biol* 11(2): 75-82.

Twombly, V., Blackman, R. K., Jin, H., Graff, J. M., Padgett, R. W. and Gelbart, W. M. (1996) 'The TGF-beta signaling pathway is essential for Drosophila oogenesis', *Development* 122(5): 1555-65.

Tzolovsky, G., Deng, W. M., Schlitt, T. and Bownes, M. (1999) 'The function of the broad-complex during Drosophila melanogaster oogenesis', *Genetics* 153(3): 1371-83.

Vuilleumier, R., Springhorn, A., Patterson, L., Koidl, S., Hammerschmidt, M., Affolter, M. and Pyrowolakis, G. (2010) 'Control of Dpp morphogen signalling by a secreted feedback regulator', *Nat Cell Biol* 12(6): 611-7.

Wang, P. Y., Chang, W. L. and Pai, L. M. (2008) 'Smiling Gurken gradient: An expansion of the Gurken gradient', *Fly (Austin)* 2(3): 118-20.

Wang, X., Bo, J., Bridges, T., Dugan, K. D., Pan, T. C., Chodosh, L. A. and Montell, D. J. (2006) 'Analysis of cell migration using whole-genome expression profiling of migratory cells in the Drosophila ovary', *Dev Cell* 10(4): 483-95.

Wu, M. Y. and Hill, C. S. (2009) 'Tgf-beta superfamily signaling in embryonic development and homeostasis', *Dev Cell* 16(3): 329-43.

Xu, T. and Rubin, G. M. (1993) 'Analysis of genetic mosaics in developing and adult Drosophila tissues', *Development (Cambridge, England)* 117(4): 1223.

Yakoby, N., Bristow, C. A., Gong, D., Schafer, X., Lembong, J., Zartman, J. J., Halfon, M. S., Schupbach, T. and Shvartsman, S. Y. (2008a) 'A combinatorial code for pattern formation in Drosophila oogenesis', *Dev Cell* 15(5): 725.

Yakoby, N., Lembong, J., Schupbach, T. and Shvartsman, S. Y. (2008b) 'Drosophila eggshell is patterned by sequential action of feedforward and feedback loops', *Development (Cambridge, England)* 135(2): 343.

Yan, D., Wu, Y., Feng, Y., Lin, S. C. and Lin, X. (2009) 'The core protein of glypican Dally-like determines its biphasic activity in wingless morphogen signaling', *Dev Cell* 17(4): 470-81.